

the photopion experiment. The ratio of the squares of electromagnetic transition form factors to the  $2^+$  and  $0^+$  states in  ${}^6\text{Li}$  at the momentum transfer corresponding to radiative pion capture is  $0.22 \pm 0.08$  (Refs. 5 and 6), again confirming the close relation between the axial and magnetic form factors.

We gratefully acknowledge the support of SIN under the directorate of Professor J. P. Blaser. This research was also supported by the German Federal Ministry for Research and Technology (BMFT) and the Swiss National Science Foundation.

<sup>1</sup>J. Hüfner, Phys. Rep. 21C, 1 (1975).

<sup>2</sup>For a review of previous experimental and theoretical work, see H. W. Baer, K. M. Crowe, and P. Truöl, Advan. Nucl. Phys. 9, 177 (1977).

<sup>3</sup>W. W. Sapp *et al.*, Phys. Rev. C 5, 690 (1972).

<sup>4</sup>J. P. Deutsch *et al.*, Phys. Lett. 26B, 315 (1968).

<sup>5</sup>J. C. Bergström, I. P. Auer, and R. S. Hicks, Nucl. Phys. A251, 401 (1975).

<sup>6</sup>R. Neuhausen and R. M. Hutcheon, Nucl. Phys. A164,

497 (1971).

<sup>7</sup>G. Audit *et al.*, Phys. Rev. C 15, 1415 (1977).

<sup>8</sup>F. Ajzenberg-Selove and T. Lauritsen, Nucl. Phys. A227, 1 (1974).

<sup>9</sup>J. C. Alder *et al.*, to be published.

<sup>10</sup>We thank K. Crowe and J. A. Bistirlich (Berkeley) and C. Tzara and N. de Botton (Saclay) for the generous loan of their targets.

<sup>11</sup>F. Ajzenberg-Selove, J. W. Watson, and R. Middleton, Phys. Rev. 139, B592 (1965).

<sup>12</sup>G. Backenstoss *et al.*, Nucl. Phys. B66, 125 (1973).

<sup>13</sup>J. B. Cammarata and T. W. Donnelly, Nucl. Phys. A267, 365 (1976).

<sup>14</sup>J. Delorme, Nucl. Phys. B19, 573 (1970).

<sup>15</sup>M. Ericson and M. Rho, Phys. Rep. 5C, 58 (1975).

<sup>16</sup>J. D. Vergados, Nucl. Phys. A220, 259 (1974).

<sup>17</sup>G. E. Dogotar *et al.*, Nucl. Phys. A282, 474 (1977); Dubna Report No. JINR E2-10509, 1977 (unpublished).

<sup>18</sup>J. D. Vergados and H. W. Baer, Phys. Lett. 41B, 560 (1972).

<sup>19</sup>J. C. Bergström, personal communication to H. W. Baer.

<sup>20</sup>W. Maguire and C. Werntz, Nucl. Phys. A205, 211 (1973).

<sup>21</sup>F. Roig and P. Pascual, Nucl. Phys. B66, 173 (1973).

<sup>22</sup>J. Delorme, M. Ericson, and G. Fäldt, Nucl. Phys. A240, 493 (1975).

## Rotational Bands in Asymmetrically Deformed ${}^{231}\text{Th}$

J. Blons, C. Mazur, D. Paya, and M. Ribrag

*Département de Physique Nucléaire, Centre d'Etudes Nucléaires de Saclay, 91190 Gif-sur-Yvette, France*

and

H. Weigmann

*Central Bureau for Nuclear Measurements, EURATOM, Geel, Belgium*

(Received 7 August 1978)

The neutron-induced fission cross section of  ${}^{230}\text{Th}$  near 720 keV is resolved into sharp structures interpreted as two rotational bands with opposite parities, indicating an asymmetrically deformed third minimum in the fission barrier.

The  ${}^{230}\text{Th}(n, f)$  cross section has long been known to exhibit a well-isolated peak at 720 keV neutron energy with a full width at half maximum (FWHM) of 35 keV. It was interpreted as a pure vibrational state in the secondary minimum of the Strutinsky potential-energy curve. From angular distribution considerations, an intrinsic state with  $K = \frac{1}{2}$  was associated with this vibration and assumed to be the head of a rotational band. Equally good fits to the data were obtained for  $K = \frac{1}{2}^+$  and  $K = \frac{1}{2}^-$ .<sup>1,2</sup> In addition, since no individual level was observed across the peak, it was difficult to deduce the moment of inertia and the de-

coupling parameter.

On the other hand, our measurements of the  ${}^{232}\text{Th}(n, f)$  cross section showed a fine structure in the peak at 1.6 MeV neutron energy, which we interpreted as a rotational band in a shallow third minimum of the potential energy curve.<sup>3</sup> From intensity considerations it was necessary to assume that both positive and negative parities were present.<sup>4</sup> In fact, the presence of two close-lying rotational bands with opposite parities can be understood as being a consequence of the asymmetric deformation expected for the third minimum<sup>5,6</sup>: The wave functions of stationary states

in a potential with two minima at nonzero values of  $\epsilon_3$  can be odd or even with respect to reflection; i.e., levels at the third minimum would split into close-lying doublets with opposite parities. In view of these questions we decided to perform a high-resolution measurement of the  $^{230}\text{Th}(n, f)$  cross section.

The electron linear accelerator at the Central Bureau for Nuclear Measurements was used as a neutron time-of-flight spectrometer with a nominal resolution of 84 psec/m. Thus at 720 keV neutron energy, the effective energy resolution was 1.7 keV (FWHM). The fission detector was a six-cell gas scintillator similar to the one previously used for the  $^{232}\text{Th}$  fission experiment. The shape of the neutron spectrum was deduced from the well-known fission cross section of  $^{237}\text{Np}$  [ENDF/B-IV (Evaluated Nuclear Data File, Version B-IV)] which was contained in one of the six cells. The absolute cross section is obtained by normalizing to a value of  $\sigma_f = 371$  mb at 1.4 MeV neutron energy.<sup>1</sup>

The fission cross section in the neighborhood of the 720-keV resonance is shown in Fig. 1. A decomposition of the vibrational resonance into eight more or less well-separated components is observed. These are too many to be explained by a single  $K = \frac{1}{2}$  rotational band and their spacings do not fit in this scheme. We thus tentatively adopt the model of an asymmetrically deformed third minimum with positive- and negative-parity rotational bands. A least-squares fit of the experimental points with a superposition of Breit-Wigner-shaped resonance curves is also shown as a full line in Fig. 1. No more than eight resonances are needed to get an extremely good fit, but a rapid deterioration is observed when less components are used. The eight components are

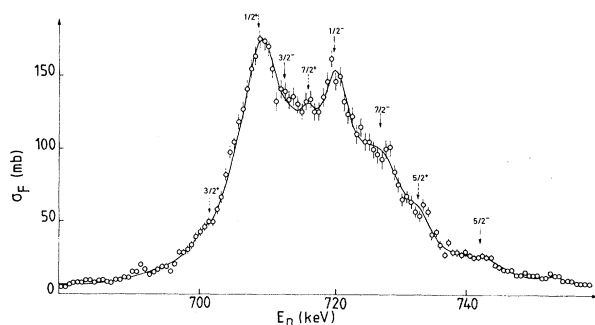


FIG. 1. Least-squares fit of the  $^{230}\text{Th}(n, f)$  experimental cross section near the 720-keV vibrational resonance.

interpreted as rotational levels and their energies, as obtained from the fit, are listed in Table I. If the energies are written in the standard form for a  $K = \frac{1}{2}$  rotational band,

$$E(J) = E_0 + \frac{\hbar^2}{2\mathcal{I}} [J(J+1) - K(K+1) + a(-1)^{J+1/2}(J + \frac{1}{2})],$$

the rotational parameters are  $\hbar^2/2\mathcal{I} = 1.90 \pm 0.06$  keV and  $a = -2.28 \pm 0.10$ , with spin assignments listed in Table I. Also given in this table are the energies calculated with the above parameters.

Values in Table I deserve several comments: (a) Although no detailed comparison has been performed with the angular distributions, a good qualitative agreement can be reached with the spins of Table I. (b) The value of  $\hbar^2/2\mathcal{I}$  and  $a$  are the same (within the error bars) for the two rotational bands. (c) The moment-of-inertia value is 3 times larger than the one of the ground-state band in the first well, whereas Specht *et al.*<sup>7</sup> found a factor of 2 between the second and the first wells. This implies, in our case, a larger deformation for the nucleus. (d) The separation of positive- and negative-parity levels is constant:

$$\Delta E^\pm = 10.8 \text{ keV}$$

(the parity determination is made on the basis of the intensities of the different components). This value of  $\Delta E^\pm$  is reasonable, as verified by a WKB calculation. It can be found with the following parameters of the  $\epsilon_3$ -dependent potential:  $\hbar\omega = 0.8$  MeV (curvature of the two minima),  $\hbar\omega_0 = 0.6$  MeV (curvature of the intermediate maximum),  $\delta E = 1$  MeV (difference between maximum and minima).

In order to show that the interpretation of the observed structure in terms of the assumed rotational bands is possible with physically reason-

TABLE I. Experimental and calculated energies for rotational bands.

$E_{\text{expt}}$ (keV)	$J^\pi$	$E_{\text{calc}}$ (keV)
$719.8 \pm 0.6$	$1/2^-$	719.7
$712.3 \pm 1$	$3/2^-$	712.4
$743.3 \pm 1$	$5/2^-$	743.6
$726.6 \pm 1$	$7/2^-$	726.6
$708.6 \pm 0.6$	$1/2^+$	708.7
$701.6 \pm 1$	$3/2^+$	701.4
$733.0 \pm 1$	$5/2^+$	732.6
$715.5 \pm 1$	$7/2^+$	715.6

TABLE II. Compound-nucleus formation cross sections  $\sigma_{CN}(J^\pi)$  and the transmission coefficients  $T_n(J^\pi)$ .

$J^\pi$	$\sigma_{CN}$ (mb)	$T_n$
$1/2^-$	700	2
$3/2^-$	1400	3.7
$5/2^-$	250	4
$7/2^-$	330	2
$1/2^+$	490	1.5
$3/2^+$	240	2.6
$5/2^+$	350	4
$7/2^+$	50	1

able reaction parameters, we have calculated a theoretical cross section for comparison with the experimental data. The calculated cross section is obtained as

$$\sigma_f(\text{calc}) = \sum_{J^\pi} \sigma_{CN}(J^\pi) \frac{T_f(J^\pi)}{T_n(J^\pi) + T_\gamma + T_f(J^\pi)}.$$

The compound-nucleus formation cross sections  $\sigma_{CN}(J^\pi)$  and the transmission coefficients  $T_n(J^\pi)$  for neutron decay (including inelastic scattering to 10 levels in  $^{230}\text{Th}$ ) have been calculated by the code FISHINGA<sup>8</sup> and are listed in Table II. According to Ref. 6 the first of the three barrier maxima is very low, and so the transmission coefficients  $T_f(J^\pi)$  may be calculated by a double-humped-fission-barrier program.<sup>8</sup> The intermediate well of the barrier has been assumed shallow such that the transmission coefficients exhibit only one subthreshold vibrational resonance. The barrier parameters for the rotational band heads ( $J = \frac{1}{2}^-$  and  $J = \frac{1}{2}^+$ ) are given in Table III. The barriers corresponding to the levels of each band are assumed to be identical except that the energies are shifted by the energy interval between the level and the band head. The calculated cross section is shown in Fig. 2. Comparison with Fig. 1 shows that the experimental fission cross section is reasonably well reproduced by the calculation although the agreement is not so perfect as it is with the fitted curve of

TABLE III. The barrier parameters for the rotational band heads.

$J^\pi$	$E_B$ (MeV)	$E_{III}$ (MeV)	$E_C$ (MeV)	$\hbar\omega_B$ (keV)	$\hbar\omega_{III}$ (keV)	$\hbar\omega_C$ (keV)
$1/2^-$	6.036	5.623	6.206	460	510	460
$1/2^+$	6.050	5.610	6.210	460	510	460

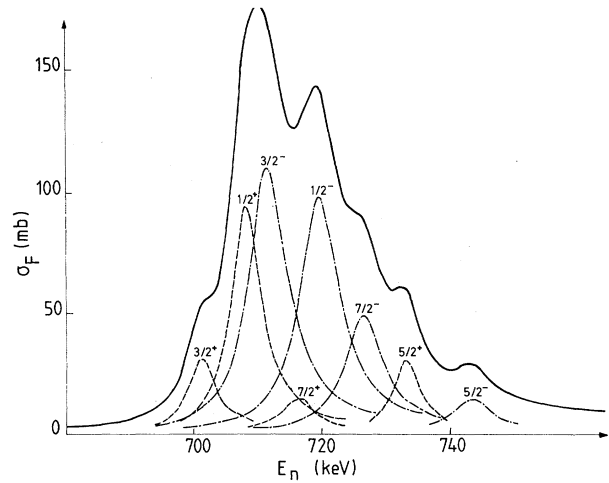
FIG. 2.  $^{230}\text{Th}(n, f)$  calculated cross section showing different components of the two rotational bands.

Fig. 1. This happens because in Fig. 1 the energy, the width, and the amplitude of each individual Breit-Wigner component were independently adjusted so as to give the best possible fit to the experimental data. On the contrary, in Fig. 2 such a fit was not tried; the energies derive from Table I, the widths are taken constant, and the relative amplitudes result from the calculated values of  $\sigma_{CN}(J^\pi)$  and  $T_n(J^\pi)$ .

It thus appears that two rotational bands with the same  $K$  value, same moment of inertia, and same decoupling parameter are present in the 720-keV peak of the  $^{230}\text{Th}$  fission cross section. Similar results are also found in the 1.6-MeV structure of the  $^{232}\text{Th}$  fission cross section.<sup>9</sup> In both cases the widths of the individual levels are too narrow (about 7 keV) to be interpreted as collective states in the second well of the potential barrier, at least if the second well is about 4 MeV deep as obtained in most calculations.<sup>8</sup> An alternative location would be the third well.<sup>5,6</sup> This interpretation is supported by the value of the moment of inertia which lies close to the calculated value in the third well<sup>10</sup> and by the presence of two parities which reflects the planar asymmetry, a characteristic feature of the third well.

We want to thank Dr. R. Joly and Dr. M. Martinot for their continuous interest in this work. Fruitful suggestions and discussions with H. Nifenecker and with Professor A. Bohr, Professor B. Mottelson, and Professor S. G. Nilsson are gratefully acknowledged.

<sup>1</sup>G. D. James, J. E. Lynn, and L. G. Earwaker, Nucl.

Phys. **A189**, 225 (1972).

<sup>2</sup>G. Yuen, G. T. Rizzo, A. N. Behkami, and J. R. Huizenga, Nucl. Phys. **A171**, 614 (1971).

<sup>3</sup>J. Blons, C. Mazur, and D. Paya, Phys. Rev. Lett. **35**, 1749 (1975).

<sup>4</sup>J. Blons, C. Mazur, and D. Paya, Fourth Biennial Study Session on Nuclear Physics, La Toussuire, 28 February-4 March 1977, Institut de Physique Nucléaire Université de Lyon, Report No. LYCEN 7702 (unpub-

lished), Vol. 2, p. S1.

<sup>5</sup>P. Möller, Nucl. Phys. **A192**, 529 (1972).

<sup>6</sup>P. Möller and R. Nix, *Physics and Chemistry of Fission, 1973* (International Atomic Energy Agency, Vienna, 1974), Vol. 3, p. 103.

<sup>7</sup>H. J. Specht *et al.*, Phys. Lett. **B41**, 43 (1972).

<sup>8</sup>G. Le Coq, private communication.

<sup>9</sup>J. Blons *et al.*, to be published.

<sup>10</sup>A. Sobiczewski, private communication.

## Relevance of the Proximity Potential to Light-Ion Scattering

S. L. Tabor and D. A. Goldberg

*University of Maryland, College Park, Maryland 20742*

and

J. R. Huizenga

*University of Rochester, Rochester, New York 14627*

(Received 11 August 1978)

Because optical-model potentials are relatively well determined by light-ion elastic scattering, we have compared such potentials with the proximity potential, which was developed for heavy-ion reactions. After the real, nuclear potentials determined by  $p$ ,  $d$ ,  $^3\text{He}$ , and  $\alpha$  scattering at 30–35 MeV/amu are transformed into the universal proximity form they are rather similar to each other and are in rough agreement with a theoretical proximity potential.

The proximity-potential formalism<sup>1</sup> represents an attempt at formulating a universal ion-ion interaction, which was developed primarily for use in heavy-ion reactions. Its physical basis lies in the fact that the range of the nuclear force is short, even in comparison with nuclear dimensions. A number of comparisons<sup>1-3</sup> have recently been made between a theoretically calculated proximity potential<sup>1</sup> and that inferred from heavy-ion elastic scattering and fusion. Such comparisons are limited by the facts that heavy-ion scattering probes only the nuclear surface and that uncertainties, such as the role of dissipative forces, exist in the interpretation of the fusion data.

Because they are less strongly absorbed, light ions can probe the ion-ion potential to much closer distances. In fact, high-energy light-ion elastic scattering beyond the nuclear "rainbow angle" not only eliminates ambiguities in the Woods-Saxon optical potential,<sup>4,5</sup> but also exhibits sensitivity to the detailed radial shape of the ion-ion potential for light-projectile systems.<sup>6</sup> These considerations have led us to compare light-ion optical potentials with the universal proximity potential, even though the latter was developed for heavy-ion reactions and uses some

large-mass approximations. It was hoped that this comparison would explore the validity of the proximity-force formalism for light ions and possibly provide experimental information on the universal proximity potential.

Blocki *et al.*<sup>1</sup> have shown that for thin-skinned matter distributions the real part of the nuclear ion-ion potential  $V_N$  is given by

$$V_N(\xi) = 4\pi\gamma b \frac{C_T C_P}{C_T + C_P} \Phi(\xi), \quad (1)$$

where  $\gamma = 0.9517\{1 - 1.7826[(N_T + N_P - Z_T - Z_P)/(A_T + A_P)]^2\}$ .  $C_i$  ( $C_P$  and  $C_T$ ) are approximately the half-density nuclear radii, which are calculated from the equivalent sharp radii according to

$$R_i = 1.28A_i^{1/3} - 0.76 + 0.8A_i^{-1/3}$$

and

$$C_i = R_i [1 - (b/R_i)^2 + \dots], \quad (2)$$

where  $b$  is a constant related to the surface diffuseness with a value<sup>7</sup> of approximately 1 fm. Because the proximity formalism emphasizes the short-range nature of the nuclear force,  $\Phi$  is conveniently expressed as a function of the separation distance  $\xi$  between the half-density